How Sodium Chloride Extends Lifetime of Bulk Nanobubbles in Water

Muye Feng,[1,∇] Xiaotong Ma,[1,∇] Zeyun Zhang,[1] Kai H. Luo,[2] Chao Sun,[1,*] Xuefei Xu[1,*]

[1]*Center for Combustion Energy, Key Laboratory of Thermal Science and Power Engineering of Ministry of Education, Department of Energy and Power Engineering, Tsinghua University, Beijing 100084, China*

[2]*Department of Mechanical Engineering, University College London, Torrington Place, London WC1E 7JE, UK*

[∇]These authors contributed equally to this work.

[*]Corresponding Author

E-mail: Chao Sun: chaosun@tsinghua.edu.cn; Xuefei Xu: xuxuefei@tsinghua.edu.cn

ABSTRACT: We present a molecular dynamics simulation study on the effects of sodium chloride addition on stability of a nitrogen bulk nanobubble in water. We find that the lifetime of the bulk nanobubble is extended in the presence of NaCl and reveal the underlying mechanisms. We do not observe spontaneous accumulation or specific arrangement of ions/charges around the nanobubble. Importantly, we quantitatively show that the N_2 molecule selectively diffuses through water molecules rather than pass by any ions after it leaves the nanobubble due to the much weaker water-water interactions than ion-water interactions. The strong ion-water interactions cause hydration effects and disrupt hydrogen bond networks in water, which leave fewer favorable paths for the diffusion of N_2 molecules, and by that reduce the degree of freedom in the dissolution of the nanobubble and prolong its lifetime. These results demonstrate that the hydration of ions plays an important role in stability of the bulk nanobubble by affecting the dynamics of hydrogen bonds and the diffusion properties of the system, which further confirm and interpret the selective diffusion path of N_2 molecules and the extension of lifetime of the nanobubble. The new atomistic insights obtained from the present research could potentially benefit the practical application of bulk nanobubbles.

KEYWORDS: bulk nanobubble; sodium chloride; stability; molecular dynamics; diffusion; ion hydration

1. Introduction

Nanobubbles are submicron gas bubbles that form both on immersed solid substrates and in aqueous solutions[1–3]. Research on nanobubbles has been attracting increasing interest in the past two decades due to their potential application in a wide range of areas including water treatment[4], medical imaging[5], froth flotation[6], agriculture breeding[7], and fuels[8]. According to the classical Young–Laplace equation and Epstein–Plesset theory[9], the massive Laplace pressure inside the nanobubble would lead to its dissolution in microseconds. However, experimental studies reported that nanobubbles could survive for hours, days, and even months[1,3,10–12]. It is widely acknowledged that the stability of surface nanobubbles results from the contact line pinning and local gas supersaturation based on the previous theoretical[13,14], experimental[15–17], and computational[18–20] studies, whereas whether or not nanobubbles can be stabilized in bulk solutions remains controversial owing to a lack of direct evidence of existence of bulk nanobubbles. Various mechanisms were proposed to rationalize the stability of bulk nanobubbles, including organic contaminant skin[21], strong hydrogen bonds[22], anomalous surface tension[23], high inner gas density[24], and charge enrichment on nanobubble surface[25–27]. But none of these mechanisms has been universally acknowledged.

The stability of bulk nanobubbles is affected by many factors, especially properties of the solution, such as temperature, pH, ionic strength, electrolyte type, surface tension, and presence of surfactants or impurities. A number of studies showed that the bulk nanobubbles are more stable in the alkaline solution due to the adsorption of hydroxyl ions,

which exerts an electrostatic pressure to balance the internal Laplace pressure, reducing gas dissolution and increasing the lifetime of the bulk nanobubbles[12,27–29]. Besides, it was reported that the lifetime of gas bubbles could be extended by the surfactants that lower the surface tension and decrease the pressure difference between the inside and outside of the bubble[30–32]. Li *et al.*[33] explored the temperature-sensitive nature of bulk nanobubbles and found that the bulk nanobubbles not only survive over a wide range of temperatures, but also tend to be more stable at higher temperatures explained by a charge-stabilization mechanism. Seddon *et al.*[34] suggested that the electrolytes could extend the lifetime of bulk nanobubbles probably through ionic shielding and/or diffusive shielding. In fact, the accumulated charges near the gas-liquid interface and ions in the bulk solutions may play a crucial role in stability of the bulk nanobubbles, which could be changed by the addition of electrolytes. Hence, the effects of electrolyte solutions with different ion valences and ionic strengths on stability of the bulk nanobubbles were intensively investigated[23,26–28,35–38], among which, NaCl, as a common monovalent electrolyte, was normally included. It was concluded that the elevated NaCl concentration reduces the thickness of the diffused electrical double layer and the magnitude of zeta potential, which leads to lower repulsion thus increases coalescence between the bulk nanobubbles. Nevertheless, understanding of how exactly ions or charges are distributed and affect stability of the bulk nanobubbles is very limited.

In addition to the above experimental work, molecular dynamics (MD) simulations were also employed to study the stability of nanobubbles. Liu and Zhang[19] indicated that

the surface nanobubbles can be stabilized in superheated or gas supersaturated liquid as a result of contact line pinning caused by the geometrical heterogeneity. Maheshwari *et al.*[20] studied the stability and growth or dissolution of a single surface nanobubble and revealed how pinning of the three-phase contact line and gas oversaturation can contribute to the stability of surface nanobubble. Weijs *et al.*[39] investigated the nucleation and stability of bulk nanobubble clusters and found that the bulk nanobubbles are stable against dissolution as long as the bubble-bubble interspacing is small enough. However, the majority of the previous MD studies on nanobubbles adopted simple LJ particles instead of all-atom model to balance the computational cost, which inevitably lost some important information at the atomistic level. In any case, a MD study on the effects of electrolyte addition on stability of the bulk nanobubbles is still lacking, leaving a knowledge gap about the underlying mechanisms.

In this paper, we use all-atom MD simulations to study the effects of NaCl addition on stability of a N_2 bulk nanobubble in water. The high spatiotemporal resolution of MD simulation makes it an ideal and powerful approach for studying the stability of bulk nanobubbles. It enables us to gain atomistic insights into the structure and dynamics of one single bulk nanobubble that may not be accessible by either experimental or continuum numerical methods. For analysis of the results, we explain the observation primarily from the perspective of diffusion throughout the paper.

2. Methods

We perform MD simulations of a bulk N_2 nanobubble in pure water and in water with

various NaCl concentrations. The details of each simulation configuration are summarized in Table 1. N_2 is chosen as the representative gas for nanobubble since it is the major constituent of air. The large NaCl concentrations are used to circumvent the high computational cost of MD simulations. The initial simulation system, as shown in Fig. 1, consists of a 7 nm diameter N_2 nanobubble placed at the center of a 14 × 14 × 14 nm^3 simulation box, and the rest of the box is filled with NaCl solution. This nanobubble configuration relates to an initial gas pressure of about 160 bar, which is designed based on results of our preliminary tests that the density of the relaxed nanobubble is higher.

Table 1. Configuration details of the studied simulation systems.

System	No. of N_2	No. of H_2O	No. of Na^+/Cl^-	NaCl concentration (mol/L)
1	700	85542	0	0
2			770	0.5
3			1540	1
4			3080	2
5			5390	3.5
6			7700	5

All of the MD simulations are performed under the isothermal-isobaric (NPT) ensemble at 298 K and 1 atm using the LAMMPS package[40]. The interatomic interactions are described by the 12-6 Lennard-Jones and Coulombic potentials with a cutoff distance of 1 nm. Long-range Coulombic interactions are computed by the particle-particle particle-mesh (PPPM) solver. Details of the potential parameters are given in Table S1 in the

Supporting Information. The N-N and O-H bonds, and the H-O-H angles within the system are kept rigid during the simulation by the SHAKE algorithm. Periodic boundary conditions are applied in all three directions. A time step of 1 fs is employed in the present study, as it is proven to be sufficient to resolve the dynamics of the system (see results of the test on different time steps in Fig. S1 in the Supporting Information). The simulation results are outputted every 10 ps. The visualization of MD simulation data is produced using OVITO[41].

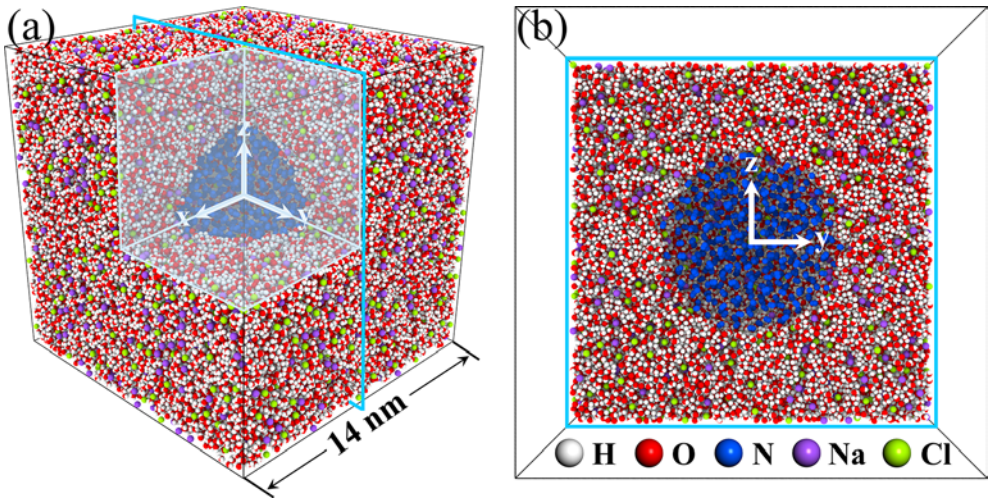

Figure 1. (a) Three-dimensional and (b) central cross-sectional views of a typical initial simulation system. One eighth of the actual simulation system in (a) is removed for a better view.

In addition to the above MD simulations, density functional theory (DFT) calculations are also performed to investigate the interaction energy between various pairs of isolated molecules involved in the present study, which provide additional insights into the results obtained from MD simulations. The DFT calculations are carried out with the def2-TZVP

basis set[42] in Gaussian 16[43]. B3LYP functional[44,45] is selected because of its excellent performance on describing noncovalent interactions. The D3 version of Grimme's dispersion with Becke-Johnson damping[46] is applied using the default parameters.

3. Results and discussion

3.1. Stability of the bulk nanobubble

First of all, a comparison is made between the dynamic behaviors of the aforementioned N_2 bulk nanobubble and a O_2 bulk nanobubble in pure water (see Fig. S2 in the Supporting Information) to examine the difference if N_2 is replaced by O_2, which is the other major constituent of air. The results are similar but the dissolution of the O_2 bulk nanobubble is faster than that of the N_2 bulk nanobubble. This is reasonable as O_2 has a better solubility than N_2 in water (approximately 41 and 18 mg/kg for O_2 and N_2 at 298 K and 1 atm[47], respectively).

Therefore, next we use a N_2 bulk nanobubble as a representative to study the effects of NaCl addition on stability of the bulk nanobubble in water. To this end, we monitor the number of N_2 molecules in the nanobubble during the 10 ns simulation. For a gas-saturated liquid, the gas oversaturation $\zeta = c_\infty/c_s - 1$ (where c_∞ is the gas concentration far away from the bubble and c_s is the gas saturation concentration) should be 0. Based on the N_2 solubility in water and the number of water molecules in the simulation system as mentioned above, the system is oversaturated if one or more than one N_2 molecules in the nanobubble diffuse into the solution, which ensures that all of our studied systems are oversaturated at a very early stage of the simulation. The ζ changes with time during the MD simulation as the

nanobubble keeps dissolving. As a result, the actual ζ in our studied systems is very high. Figure 2(a) clearly shows that the lifetime of the nanobubble is extended with the addition of NaCl and the dissolution of the nanobubble is slower as the NaCl concentration increases. An additional 10 ns simulation is carried out for the 2 mol/L NaCl case, the result of which illustrates that there is no significant change in the decay trend even if the simulation is continued. Therefore, we assume that the situation would be the same for all studied cases. Furthermore, as shown in Fig. 2(b), by tracking the diameter of the nanobubble over time, the results are found to give the same conclusion on nanobubble stability as drawn from Fig. 2(a). The reduction in the diameter of the nanobubble is slower with the increasing NaCl concentration, suggesting a more stable nanobubble. The starting diameters vary and are all smaller than the designed 7 nm because the nanobubble undergoes different levels of initial contraction caused by the relaxation of the surrounding solution. A higher NaCl concentration results in a smaller nanobubble at the beginning but a smoother dissolution process, whereas the initial diameter of the nanobubble is larger with a lower NaCl concentration but the nanobubble dissolves more rapidly. It is noteworthy that as the nanobubble keeps dissolving and does not reach equilibrium during our MD simulation, the size of the simulation box also decreases accordingly with the shrinkage of the nanobubble. As expected, the reduction in size of the simulation box is more pronounced for the system with a faster dissolution of the nanobubble.

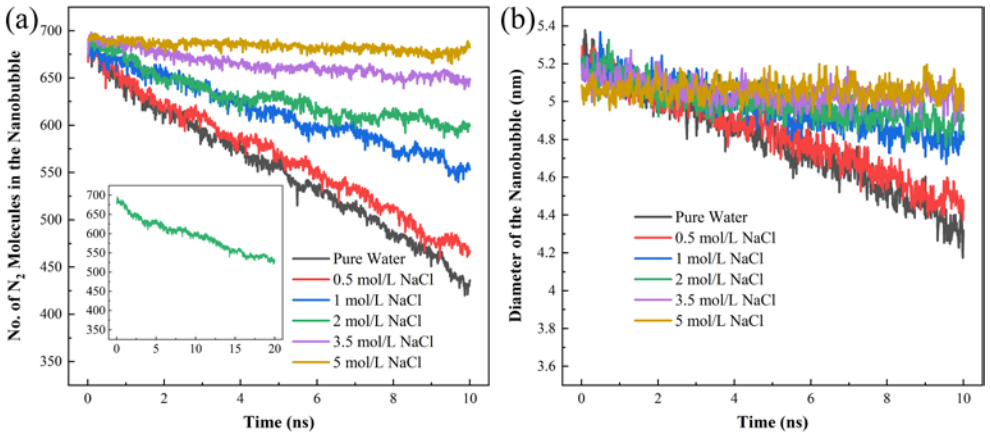

Figure 2. Time evolution of (a) the number of N_2 molecules in the nanobubble and (b) diameter of the nanobubble of all studied systems during the 10 ns MD simulations. Simulation of the 2 mol/L NaCl case in (a) is extended to 20 ns as a test case to confirm that there is no significant change in the decay trend even if the simulation is continued. Based on the fact that the shape of the nanobubble is kept fairly spherical during the simulation, the diameter of the nanobubble is calculated using the formula for the volume of a sphere, where the volume is estimated by constructing surface meshes on the nanobubble implemented in OVITO.

Table 2. Comparison between the lifetime results estimated from the MD simulation and from the EP theory.

NaCl concentration (mol/L)	Lifetime (ns)	
	MD simulation	EP theory
0	60	37
0.5	70	41
1	123	39
2	183	45
3.5	422	53
5	76003	55

By fitting the results of Fig. 2(b), the lifetimes of the nanobubble in all simulation systems are estimated based on the linear relationship (see Fig. S3 in the Supporting Information). It is noted that the studied size of the bulk nanobubble in the present MD

study is possibly below a certain critical size, beyond which the relationship between the size and time may not be simply linear and the nanobubble could be more stable. Additionally, we also determine the lifetimes of the nanobubble in all simulation systems using the Epstein-Plesset (EP) theory[9,25] for comparison:

$$\frac{dR}{dt} = -\frac{D\Delta c}{\rho}\left(\frac{1}{R} + \frac{1}{\sqrt{\pi Dt}}\right) \quad (1)$$

$$\Delta c = c_s\left(\frac{2\gamma}{RP_0} - \zeta\right) \quad (2)$$

where R is the radius of the bulk nanobubble, t is the time, D is the diffusion coefficient of dissolved gas in water, ρ is the density of gas, c_s is the gas saturation concentration, γ is the surface tension, P_0 is the atmospheric pressure, and ζ is the gas oversaturation. All data used for the calculations is provided in Table S2 in the Supporting Information. The comparison between the lifetime results estimated from the MD simulation and from the EP theory is shown in Table 2. Overall, the difference in lifetime with various NaCl concentrations of EP theory is not as significant as of MD simulation. The lifetime in the 5 mol/L system estimated from MD simulation is two orders of magnitude higher than that of the 3.5 mol/L system, which could be due to the relatively poor linear fitting that overestimates the lifetime. Similarly, an abnormal lifetime in the 1 mol/L system estimated from EP theory, which is slightly smaller than that of the 0.5 mol/L system is noticed. The anomaly could result from some specific data (*e.g.* γ and ζ) we use for calculation in Table S2. The results show that the EP theory produces comparable results with our MD simulation at low NaCl concentrations (0 and 0.5 mol/L). At higher NaCl concentrations,

the lifetimes estimated from EP theory are much lower than those from MD simulation. This could be partially attributed to the applicability of EP theory. The EP theory is based on the Fick's law, which is applicable to dilute solution. As a result, the EP theory is also applicable to dilute solution, thus may not be suitable for estimating the lifetime at high NaCl concentrations. Also, the MD estimations on lifetime at higher NaCl concentrations are not as satisfactory as those at lower ones.

We notice that the effects of NaCl addition on stability of the bulk nanobubble observed from experiments[12,26,27] are different from the results obtained from our simulations. Our MD results show that the lifetime of the bulk nanobubble is extended and the stability of the bulk nanobubble is enhanced in the presence of NaCl, whereas experimental studies[12,26,27] reported that the addition of NaCl destabilizes the bulk nanobubbles. The reason is that we study and define the stability of the bulk nanobubble from a different perspective compared with the experiment. In the experiments, the elevated NaCl concentration drives the negative zeta potential towards zero, which reduces the repulsive electrostatic forces between the bulk nanobubbles. This lower repulsion then increases the coalescence between the bulk nanobubbles. Hence, the stability of the bulk nanobubbles in experiment is actually a collective property for the population, which is estimated based on the repulsion and possibility of coalescence between the bulk nanobubbles. However, our MD study evaluates the stability of one single bulk nanobubble on the basis of its lifetime or dissolution rate by monitoring the number of gas molecules in the nanobubble and tracking the diameter of the nanobubble over time. As a consequence,

there is no contradiction between the different conclusions on stability of the bulk nanobubble drawn from the experiments and from our MD study.

3.2. Distribution of ions

As previous studies proposed a hypothesis of charge enrichment on the surface of the bulk nanobubble[25,26], we calculate the various radial density profiles, as shown in Fig. 3, to investigate if there is any preferential distribution of charges near the nanobubble. However, different from the hypothesis, no measurable accumulation or specific arrangement of ions/charges around the nanobubble is observed in the present simulations. Figure 3(a) describes a stable overall mass density within the solution region (outside the gas-liquid interface or transition area where a significant increase in density occurs), while Fig. 3(b) displays a noisy distribution of ions/charges outside the nanobubble because of fluctuations. Therefore, it is suggested that both water molecules and ions are almost randomly and uniformly distributed in the solution. The measured density of N_2 inside the nanobubble (about 344 kg/m^3, gives a gas pressure of around 400 bar) is much higher than that of gaseous N_2 at normal conditions (1.25 kg/m^3) and is of the same order of magnitude as that of liquid N_2 (807 kg/m^3), which confirms the conclusion drawn from previous studies[24,48,49]. For example, Zhou *et al.*[49] experimentally revealed that the gas density inside the nanobubble is 1-2 orders of magnitude higher than that in atmospheric pressure.

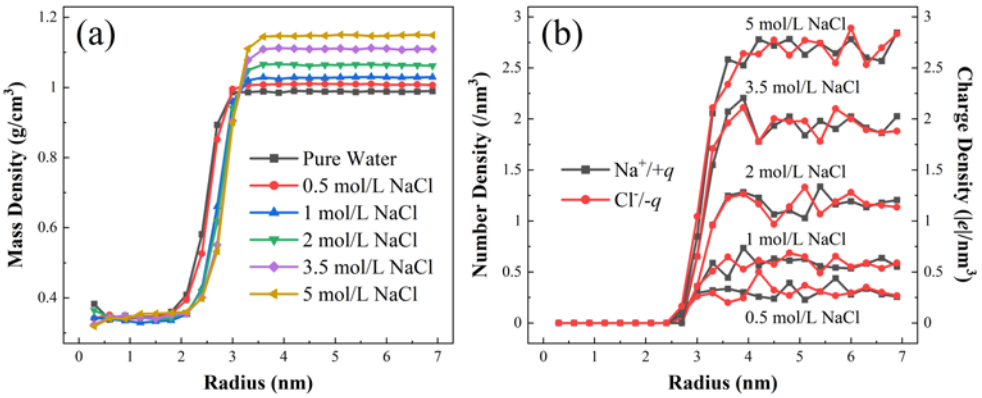

Figure 3. (a) Radial mass density profiles of all studied systems. The results are averaged over the last 1 ns (9-10 ns) of the simulation. (b) Radial number density profiles of Na^+ and Cl^-, and absolute charge density profiles of simulation systems with various NaCl concentrations. Different from (a), these are single-frame results at 10 ns to obtain instantaneous distribution. The bin size in the radial direction used for calculation is 0.3 nm. The radius starts from the center of mass of the bulk nanobubble.

Additionally, we also construct an artificial negatively charged bulk nanobubble, whose structure is similar as in the charge enrichment hypothesis, to check if the nanobubble and negative charges can be maintained during the simulation (see details in Fig. S4 in the Supporting Information). The results demonstrate that the ordered ions finally become randomly distributed during the 5 ns MD simulation. In the meantime, the nanobubble still gradually dissolves in the solution. In brief, the model of charge accumulation on nanobubble surface proposed in previous studies[25,26] is not observed and cannot be stabilized based on our MD simulations. An ideal system simply composed of the N_2 bulk nanobubble, water, and NaCl, without considering other factors such as impurities or surfactants, would not present the phenomenon of charge accumulation on the nanobubble surface. The exact reason for the reported charge accumulation needs further studies.

The nearly random distribution of ions in water rather than charge enrichment on the surface of the bulk nanobubble could be explained by the position of Na^+ and Cl^- in the well-known Hofmeister Series[50]. According to the Hofmeister Series, ions can be classified as kosmotropes or chaotropes. Kosmotropes (so-called water structure makers) are small ions with high charge densities having a strong ability to disrupt the hydrogen bond networks among water molecules, whereas chaotropes (so-called water structure breakers) are large ions with low charge densities and are less/unable to break the hydrogen bonds so the surrounding water molecules tend to retain their hydrogen-bonded pattern[51]. Based on changes in the ion hydration free energy between the bulk and the interface[52–54], kosmotropic ions prefer the bulk water, where they can be better hydrated, while chaotropic ions are expelled from the bulk water towards the interface, where there are fewer water molecules. NaCl was found to be a "Hofmeister neutral" salt[55], which means both Na^+ and Cl^- are nearly neutral in the Hofmeister Series[50,56–58], *i.e.* Na^+ is only marginally kosmotropic and Cl^- is only marginally chaotropic. Figure 4 illustrates the hydration of Na^+ and Cl^- observed in the MD simulations. The radial distribution functions (RDF) of ion-oxygen and water coordination numbers of ions at various NaCl concentrations can be seen in Fig. 5, both of which are in good accordance with previous studies[59–61]. Consistent with the neutrality of Na^+ and Cl^- in the Hofmeister Series, the results indicate that Na^+ and Cl^- have a similar hydration ability as the difference in their water coordination numbers are small (no more than 1.6) at the same concentration. Therefore, the close proximity between Na^+ and Cl^- in the Hofmeister Series would not lead to clear ion/charge accumulation on

nanobubble surface. But it could be expected that an alternative salt with a combination of a highly kosmotropic ion and a highly chaotropic ion is likely to show distinctly different ion distributions in the bulk water and on the surface of the nanobubble.

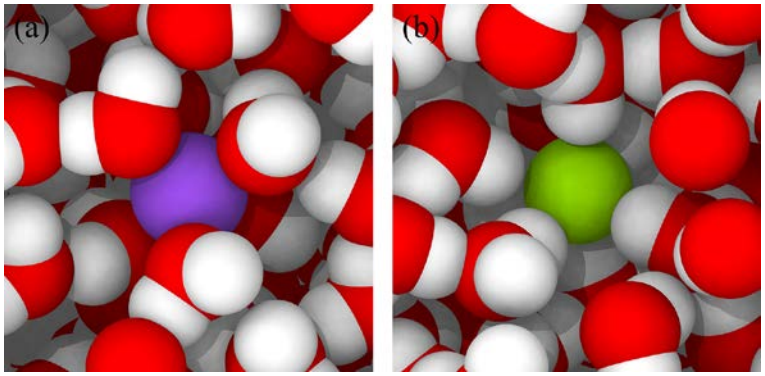

Figure 4. Snapshots of (a) hydration of Na^+ (surrounded by O atoms of H_2O molecules) and (b) hydration of Cl^- (surrounded by H atoms of H_2O molecules).

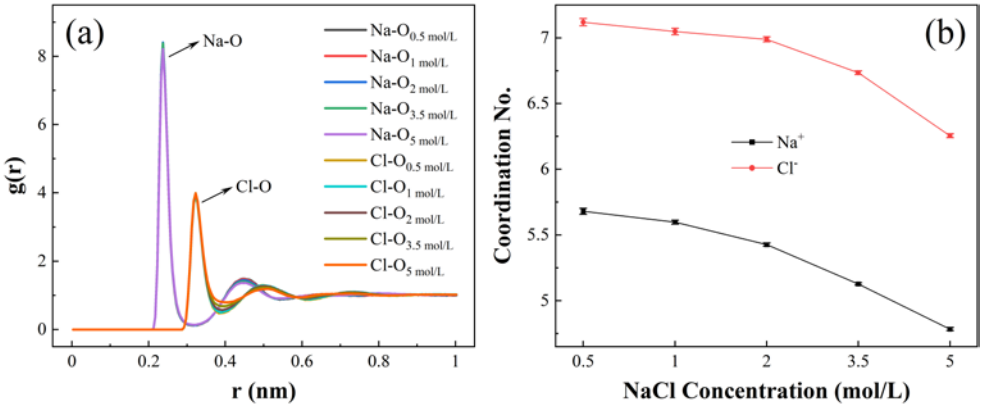

Figure 5. (a) Radial distribution functions (RDF) of ion-oxygen and (b) water coordination numbers of ions at various NaCl concentrations. The results are averaged over the last 1 ns (9-10 ns) of the simulation. The bin size used for RDF calculation is 0.005 nm. The cutoff values ($r_{Na\text{-}O}$ and $r_{Cl\text{-}O}$) used for coordination number calculation are determined from the first minimum in the RDF (see Table S3 in the Supporting Information). A water molecule is considered as being coordinated to the ion if the distance of ion-oxygen $r_{ion\text{-}oxygen} \leq r_{cutoff}$.

To sum up, the difference in arrangement of ions/charges between our MD and previous experimental results could be attributed to factors such as impurities or surfactants,

which are not involved in our MD study, and the nearly random distribution of ions in water could be explained by the close proximity between Na^+ and Cl^- in the Hofmeister Series. Both of these two topics are worthy of in-depth future studies.

3.3. Diffusion properties of the system

3.3.1. Selective diffusion path of N_2 molecules

Why can the NaCl addition extend the lifetime of the nanobubble in water? We start from studying the simulation trajectory, especially the way that a N_2 molecule leaves the nanobubble. Interestingly, it seems that the N_2 molecule always chooses to walk through a waterway rather than pass by any ions when it departs from the nanobubble. The subsequent diffusion path of the N_2 molecule in the solution is also surrounded by water molecules. To quantify and confirm our observation, we investigate the surrounding environment of all free N_2 molecules outside the nanobubble by counting the number of those free N_2 molecules (N_{N_2}), and the number of Na^+, Cl^- and H_2O (N_{Na^+}, N_{Cl^-} and N_{H_2O}) within a specific distance (R in Fig. 6(a)) along their diffusion paths during the simulation with various NaCl concentrations, to obtain the ratio of N_{Na^+}/N_{H_2O} and N_{Cl^-}/N_{H_2O} as a function of R. All N_2 molecules are included in the calculation from the instant when they leave the nanobubble (N_{N_2} together with N_{Na^+}, N_{Cl^-} and N_{H_2O} change with time). More specifically, for every free N_2 molecule, our purpose is to determine its N_{Na^+} and N_{Cl^-} within different R during a certain period of time (see caption of Fig. 6), and then sum up all time-averaged N_{Na^+} and N_{Cl^-} for all free N_2 molecules over the R range. Finally, we calculate the $(N_{Na^+}/N_{N_2})/(N_{H_2O}/N_{N_2})$ and $(N_{Cl^-}/N_{N_2})/(N_{H_2O}/N_{N_2})$ at different R, namely N_{Na^+}/N_{H_2O} and N_{Cl^-}

/N_{H_2O} as a function of *R*.

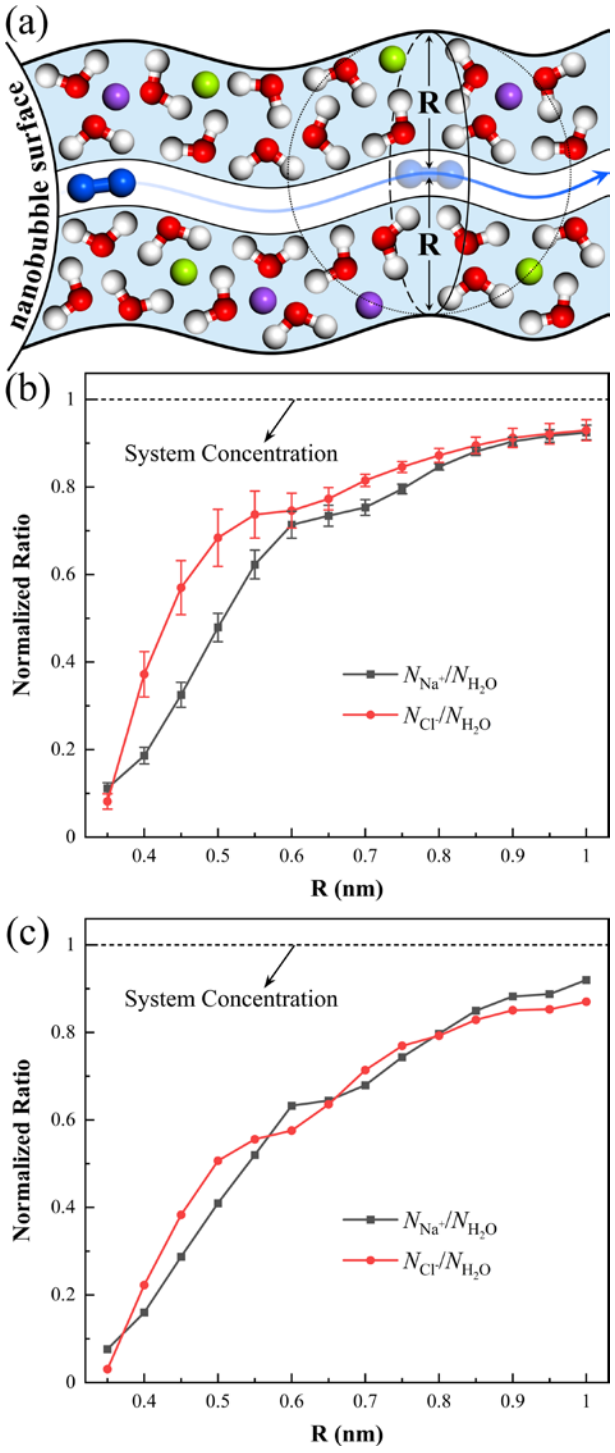

Figure 6. (a) Sketch of the diffusion path of a N_2 molecule after it leaves the nanobubble. (b) Normalized ratio between the number of two different ions and water molecules based on (a) with various NaCl concentrations. The number results are averaged over the last 1 ns (9-10 ns) of the simulation. (c) The results of (b) for a random single N_2 molecule after

it leaves the nanobubble in the system with 1 mol/L NaCl.

As can be seen in Fig. 6(b), the ionic concentration around the free N_2 molecules rises and gradually approaches the system concentration as the distance R increases, indicating that the N_2 molecules prefer a water environment with few ions from the instant when they leave the nanobubble as there are fewer ions within a closer distance to the free N_2 molecules. The tendency of the ionic concentration sufficiently demonstrates the selective diffusion path of the free N_2 molecules through water. Otherwise, the ionic concentration should remain nearly constant regardless of R. It is worth mentioning that N_{Cl^-}/N_{H_2O} is larger than N_{Na^+}/N_{H_2O} in Fig. 6(b) except the first data point at R = 0.35 nm and there is a critical point at R = 0.6 nm, from which the climbing rate of both N_{Na^+}/N_{H_2O} and N_{Cl^-}/N_{H_2O} becomes moderate. This is related to the local spatial structure network of N_2, H_2O and ionic hydration shells. In addition to the different interaction distances between Na-O and Cl-O shown in Fig. 5(a), further quantitative investigations need to be conducted to give a detailed explanation of the results. We also track a random single N_2 molecule after it leaves the nanobubble (Fig. 6(c)) and obtain the data as in Fig. 6(b). The results in the two figures show good mutual verification. As mentioned in Section 3.2, it is found that the water structure is changed and the hydrogen bond networks are broken in the presence of Na^+ and Cl^-. Consequently, the number of hydrogen bonds between water molecules in the system decreases with the increasing NaCl concentration (see Fig. S5(a) in the Supporting Information; the criteria used to identify the hydrogen bond are obtained from Ref.[62]; an

excellent linear relationship between the number of hydrogen bonds and NaCl concentration is observed in Fig. S5(b)). Briefly speaking, the N_2 molecule selectively diffuses through water molecules but the introduction of ions causes hydration effects (reduces the number of available free water molecules) and leaves fewer favorable paths for the diffusion of N_2 molecules, thus reducing the degree of freedom in the dissolution of the nanobubble.

We calculate the various interaction energies based on the employed classical force fields to further reveal the underlying cause for the selective diffusion path of N_2 molecules. To make a comparison, the same DFT calculations are also performed. As shown in Fig. 7, the interaction energies obtained from classical force fields are in good agreement with those from DFT calculations, which verifies the effectiveness of the chosen classical force fields in the present study. The interaction energy between ion (both Na^+ and Cl^-) and water molecule is much more negative than that between water molecules, indicating much stronger ion-water interactions than hydrogen-bonded water-water interactions. Undoubtedly, the N_2 molecule prefers to migrate by breaking through the weaker interaction between water molecules. This easiest choice results in the selective diffusion path of N_2 molecules through water.

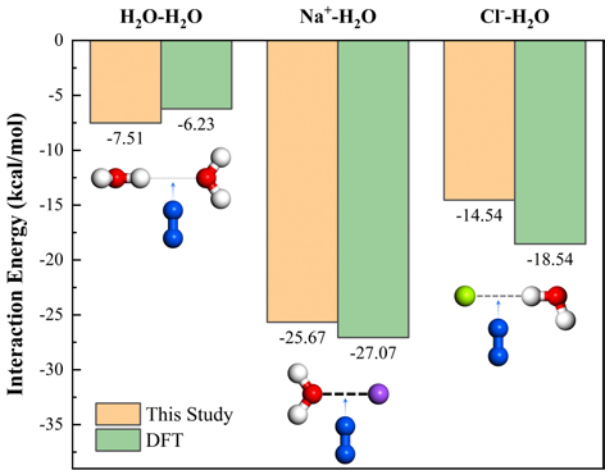

Figure 7. Interaction energies of H_2O-H_2O, Na^+-H_2O, and Cl^--H_2O obtained from the classical force fields used in this study and from DFT calculations. The interaction between water molecules is the weakest among the three, so the easiest choice for N_2 molecule is to diffuse through water molecules.

3.3.2. Effects of NaCl addition on the diffusion coefficients

Table 3. Diffusion coefficient of N_2, Na^+, Cl^-, and H_2O and system average over all studied systems.

NaCl concentrations (mol/L)	Diffusion coefficient (D, 10^{-9} m^2/s)				
	N_2	Na^+	Cl^-	H_2O	Average
0	2.37	N/A	N/A	2.71	2.71
0.5	2.15	1.17	1.44	2.52	2.51
1	2.11	1.09	1.31	2.32	2.31
2	1.62	0.88	1.16	1.93	1.91
3.5	1.27	0.72	0.90	1.52	1.49
5	1.06	0.57	0.66	1.19	1.16

Since the bulk nanobubble keeps dissolving and does not reach equilibrium, we build new small but comparable systems to better estimate the diffusion coefficients. The calculation details are provided in the Supporting Information and the results of various

diffusion coefficients are listed in Table 3. The D_{N_2} and D_{H_2O} in pure water are in good agreement with experimental results (2.01×10^{-9} m^2/s[63] and 2.30×10^{-9} m^2/s[64], respectively), verifying the effectiveness of the calculated diffusion coefficients in Table 3. As expected, D_{N_2} drops with the elevated NaCl concentration, meaning that the diffusion of N_2 thus the dissolution of the nanobubble is slower as the NaCl concentration increases, which is consistent with the effects of NaCl addition on nanobubble stability concluded in Section 3.1. In addition to D_{N_2}, D_{Na^+}, D_{Cl^-}, D_{H_2O} and $D_{Average}$ all decrease in the presence of increasingly more ions, which indicates that the diffusion of all species as well as the whole system is slower. In other words, the system is more stable if there are more ions. This is owing to the hydration effects induced by the ions. The hydration of ions reduces the number of free water molecules, which can move rapidly through the hydrogen bond network and whose motion can promote the diffusion of ions and N_2. The consequent reduction in the number of the selective diffusion path of N_2 through water further leads to the decreased D_{N_2}. As a result, the diffusion of the whole system is slowed down producing a more stable system with the addition of NaCl.

It is noted that D_{Na^+} is smaller than D_{Cl^-}, which can be explained by the stronger Na^+-H_2O than Cl^--H_2O interaction based on our DFT results. The water molecules in the ionic hydration shell exchange with the surrounding free water molecules, and this exchange activity drives the ion-water “cluster” and facilitates the diffusion of the ion. The stronger binding between Na^+ and H_2O than between Cl^- and H_2O makes this exchange activity less frequent for the Na^+-H_2O “cluster”, the diffusion resistance for which is therefore larger.

Our results of D_{Na^+} and D_{Cl^-} are comparable with those obtained in *ab initio* molecular dynamics simulations[65], where D_{Na^+} and D_{Cl^-} are 0.799×10^{-9} m^2/s and 1.215×10^{-9} m^2/s, respectively, at a NaCl concentration of 3 mol/L.

3.4. Properties of the hydrogen bond

3.4.1. Hydrogen bond at the interface and in the bulk

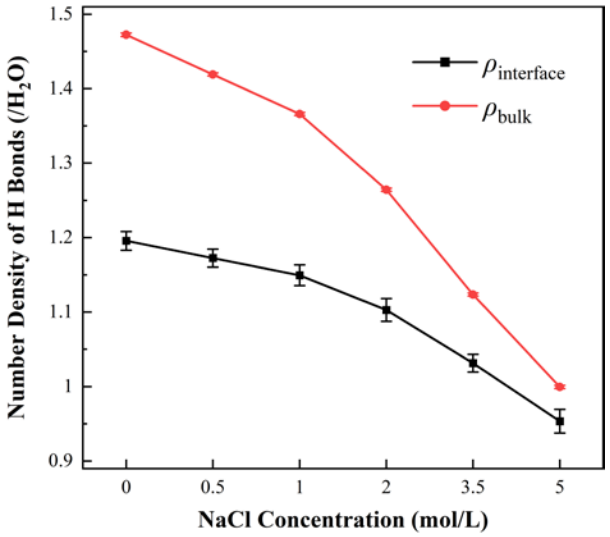

Figure 8. Number density of the hydrogen bonds (number of hydrogen bonds per water molecule) at the interface and in the bulk of all studied systems. The results are averaged over the last 1 ns (9-10 ns) of the simulation.

Figure 8 shows the number density of the hydrogen bonds at the interface ($\rho_{interface}$) and in the bulk (ρ_{bulk}) of all studied systems. The method to differentiate the interface from the bulk is provided in the Supporting Information. The difference between $\rho_{interface}$ and ρ_{bulk} regardless of NaCl concentration shown in Fig. 8 is attributed to the different orientations or structures of water molecules at the interface from those in the bulk. We use α and β shown in Fig. 9(a) to characterize the orientation of a water molecule and calculate

the radial mean α and mean β profiles, which can be seen in Fig. 9(b) and 9(c), respectively. The dipole vector is designated as ***a***, the vector of O to H is designated as ***b***, and the vector of COM (the center of mass) of the nanobubble to O is designated as ***c***. The angles between ***a*** and ***c*** and between ***b*** and ***c*** are defined as α and β, respectively. There are two OH vectors (***b***) and the larger β is chosen. It is apparent that both α and β at the interface are different from those in the bulk, demonstrating the water structure difference between the interface and the bulk. Additionally, the NaCl addition increases the maximums of both α and β at the interface. Based on the selective diffusion path of N_2 molecules through water (*i.e.* by breaking the hydrogen bond), hydrogen bond density ρ can be considered as a measurement for the difficulty level of N_2 diffusion. A higher ρ means more available diffusion paths thus easier N_2 diffusion, and *vice versa*. For both the interface and the bulk, increasing the NaCl concentration decreases hydrogen bond density ρ as more water molecules need to be coordinated with the ions, disrupting the hydrogen bond networks to a greater extent. We also notice that the gap between $\rho_{\text{interface}}$ and ρ_{bulk} narrows down with the elevated NaCl concentration. If ρ is used as an indicator to describe the spatial structure of the system, it means that the addition of NaCl reduces the structural difference between the interface and the bulk.

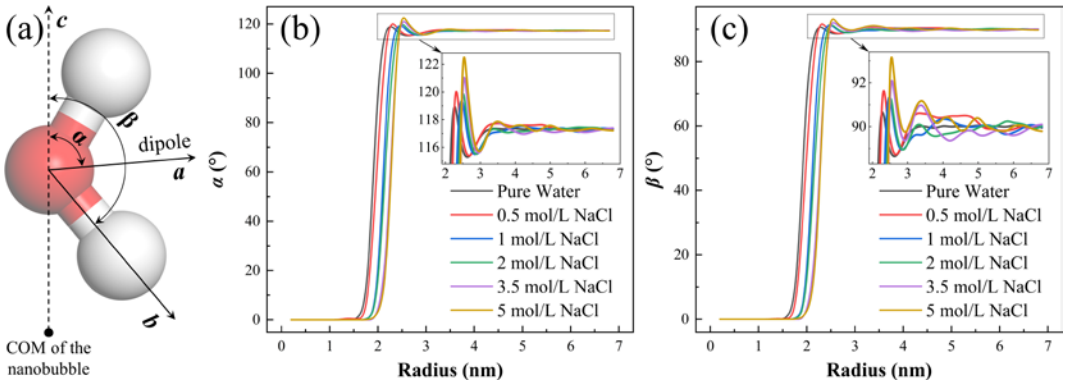

Figure 9. (a) Sketch of α and β used to characterize the orientation of a water molecule. COM is short for the center of mass. (b) Radial mean α and (c) radial mean β profiles of all studied systems. The results are averaged over the last 1 ns (9-10 ns) of the simulation. The bin size in the radial direction used for calculation is 0.2 nm. The range covered by zero at the beginning of each profile represents the nanobubble area where there are no water molecules.

3.4.2. Lifetime of the hydrogen bond

Table 4. Lifetime of the hydrogen bond of all studied systems.

NaCl concentrations (mol/L)	Hydrogen bond lifetime (τ, fs)	
	Continuous (τ_c)	Intermittent (τ_{int})
0	479	3599
0.5	474	3659
1	472	3754
2	467	3939
3.5	460	4225
5	458	4619

The hydrogen bond lifetime is calculated as described in Ref.[66]. The calculation details are provided in the Supporting Information and the results are listed in Table 4. The continuous definition measures the time that a hydrogen bond remains continuously intact,

whereas the intermittent definition allows the hydrogen bond considered broken to be subsequently reformed and counted again at a future time point. As the NaCl concentration increases, the continuous lifetime τ_c is shorter but the intermittent lifetime τ_{int} is longer. The shorter τ_c can be explained by the hydration effects of ions. The ion-water "cluster" moves as a whole and the water molecules in the ionic hydration shell exchange with the surrounding free water molecules, and the movement of the "cluster" and the exchange activity break the nearby hydrogen bonds. The increase in the number of ions affects more such kind of hydrogen bonds, leading to a shorter τ_c. The longer τ_{int} indicates that the structure between water molecules (hydrogen bond networks) or the whole system is more stable in the presence of more ions, which is consistent with the results of the diffusion coefficients. A more stable system is beneficial for extending the lifetime of the bulk nanobubble in water. Furthermore, both τ_c and τ_{int} are found to have a satisfactory linear relationship with the D_{H_2O} in Table 3 (see Fig. S6 in the Supporting Information).

4. Conclusions

A series of MD simulations are performed to investigate the effects of NaCl addition on the lifetime and stability of a N_2 bulk nanobubble in water. The results reveal that the lifetime of the bulk nanobubble can be extended and the stability of the bulk nanobubble can be enhanced with the addition of NaCl. We do not observe spontaneous accumulation or specific arrangement of ions/charges around the nanobubble in the current work. This suggests that the previously proposed model of charge accumulation on nanobubble surface may result from other unknown factors to be studied in the future. The nearly random

distribution of Na^+ and Cl^- in water rather than charge enrichment on the surface of the bulk nanobubble could be explained by the close proximity between Na^+ and Cl^- in the well-known Hofmeister Series. Our MD results validate that Na^+ and Cl^- have a similar hydration ability and therefore support the explanation.

Importantly, from the diffusion point of view, we find that the N_2 molecule selectively diffuses through water molecules rather than any pass by ions after it leaves the nanobubble. The introduction of ions causes hydration effects and breaks the hydrogen bond networks between water molecules, which leaves fewer favorable paths for the diffusion of N_2 molecules, thus reducing the degree of freedom in the dissolution of the nanobubble. Furthermore, we calculate the various interaction energies to further explain the selective diffusion path of N_2 molecules. The interaction between ion (both Na^+ and Cl^-) and water molecule is found to be much stronger than that between hydrogen-bonded water molecules. Hence, the N_2 molecule prefers to migrate by breaking through the weaker interaction between water molecules, resulting in the selective diffusion path of N_2 molecules through water. The effects of NaCl addition on the diffusion coefficients are also studied. The results show that the diffusion of the whole system is slower producing a more stable system in the presence of NaCl.

The properties of the hydrogen bond in the system are studied in detail. Although increasing the NaCl concentration decreases the number density of the hydrogen bonds ρ for both the interface and the bulk, the gap between $\rho_{\text{interface}}$ and ρ_{bulk} narrows down. We calculate the continuous lifetime τ_c and intermittent lifetime τ_{int} of the hydrogen bond and

find that τ_c is shorter but τ_{int} is longer as the NaCl concentration increases. It is suggested that the hydration of ions plays an important role in both the diffusion and hydrogen bond properties of the system, which further confirm the selective diffusion path of N_2 molecules, and finally affect the lifetime or stability of the bulk nanobubble.

The present research improves our understanding of how NaCl might affect the lifetime and stability of bulk nanobubbles in water from a microscopic viewpoint. The new findings could potentially benefit the practical application of bulk nanobubbles. For example, there may exist an ideal salt with a specific concentration that could balance the collective stability and individual stability of bulk nanobubbles in the solution, thereby optimizing their performance.

Conflicts of interest

There are no conflicts of interest to declare.

Acknowledgments

Funding from the National Natural Science Foundation of China (NSFC, Grant Nos. 11988102 and 52106164), the China Postdoctoral Science Foundation (Grant No. 2021M691728), and the UK Engineering and Physical Sciences Research Council under the project “UK Consortium on Mesoscale Engineering Sciences (UKCOMES)” (Grant No. EP/R029598/1) is gratefully acknowledged. The first author is also grateful for the support of “Shuimu Tsinghua Scholar” program from Tsinghua University.

References

(1) Lohse, D.; Zhang, X. Surface Nanobubbles and Nanodroplets. *Rev. Mod. Phys.*

2015, *87* (3), 981–1035.

(2) Zhang, X.; Lhuissier, H.; Sun, C.; Lohse, D. Surface Nanobubbles Nucleate Microdroplets. *Phys. Rev. Lett.* **2014**, *112* (14), 144503.

(3) Alheshibri, M.; Qian, J.; Jehannin, M.; Craig, V. S. J. A History of Nanobubbles. *Langmuir* **2016**, *32* (43), 11086–11100.

(4) Tang, W.W.; Zeng, G.M.; Gong, J.L.; Liu, Y.; Wang, X.Y.; Liu, Y.Y.; Liu, Z.F.; Chen, L.; Zhang, X.R.; Tu, D.Z. Simultaneous Adsorption of Atrazine and Cu (II) from Wastewater by Magnetic Multi-Walled Carbon Nanotube. *Chem. Eng. J.* **2012**, *211–212*, 470–478.

(5) Wang, Y.; Li, X.; Zhou, Y.; Huang, P.; Xu, Y. Preparation of Nanobubbles for Ultrasound Imaging and Intracelluar Drug Delivery. *Int. J. Pharm.* **2010**, *384* (1), 148–153.

(6) Azevedo, A.; Oliveira, H.; Rubio, J. Bulk Nanobubbles in the Mineral and Environmental Areas: Updating Research and Applications. *Adv. Colloid Interface Sci.* **2019**, *271*, 101992.

(7) Ahmed, A. K. A.; Shi, X.; Hua, L.; Manzueta, L.; Qing, W.; Marhaba, T.; Zhang, W. Influences of Air, Oxygen, Nitrogen, and Carbon Dioxide Nanobubbles on Seed Germination and Plant Growth. *J. Agric. Food Chem.* **2018**, *66* (20), 5117–5124.

(8) Oh, S. H.; Han, J. G.; Kim, J.M. Long-Term Stability of Hydrogen Nanobubble Fuel. *Fuel* **2015**, *158*, 399–404.

(9) Epstein, P. S.; Plesset, M. S. On the Stability of Gas Bubbles in Liquid-Gas Solutions. *J. Chem. Phys.* **1950**, *18* (11), 1505–1509.

(10) Ohgaki, K.; Khanh, N. Q.; Joden, Y.; Tsuji, A.; Nakagawa, T. Physicochemical Approach to Nanobubble Solutions. *Chem. Eng. Sci.* **2010**, *65* (3), 1296–1300.

(11) Ghaani, M. R.; Kusalik, P. G.; English, N. J. Massive Generation of Metastable Bulk Nanobubbles in Water by External Electric Fields. *Sci. Adv.* **2020**, *6* (14), eaaz0094.

(12) Nirmalkar, N.; Pacek, A. W.; Barigou, M. On the Existence and Stability of Bulk Nanobubbles. *Langmuir* **2018**, *34* (37), 10964–10973.

(13) Liu, Y.; Zhang, X. Nanobubble Stability Induced by Contact Line Pinning. *J. Chem. Phys.* **2013**, *138* (1), 14706.

(14) Lohse, D.; Zhang, X. Pinning and Gas Oversaturation Imply Stable Single Surface Nanobubbles. *Phys. Rev. E* **2015**, *91* (3), 31003.

(15) Tyrrell, J. W. G.; Attard, P. Images of Nanobubbles on Hydrophobic Surfaces and Their Interactions. *Phys. Rev. Lett.* **2001**, *87* (17), 176104.

(16) Zhang, X. H.; Quinn, A.; Ducker, W. A. Nanobubbles at the Interface between Water and a Hydrophobic Solid. *Langmuir* **2008**, *24* (9), 4756–4764.

(17) An, H.; Liu, G.; Atkin, R.; Craig, V. S. J. Surface Nanobubbles in Nonaqueous Media: Looking for Nanobubbles in DMSO, Formamide, Propylene Carbonate, Ethylammonium Nitrate, and Propylammonium Nitrate. *ACS Nano* **2015**, *9* (7), 7596–7607.

(18) Weijs, J. H.; Snoeijer, J. H.; Lohse, D. Formation of Surface Nanobubbles and the Universality of Their Contact Angles: A Molecular Dynamics Approach. *Phys. Rev. Lett.* **2012**, *108* (10), 104501.

(19) Liu, Y.; Zhang, X. A Unified Mechanism for the Stability of Surface Nanobubbles: Contact Line Pinning and Supersaturation. *J. Chem. Phys.* **2014**, *141* (13), 134702.

(20) Maheshwari, S.; van der Hoef, M.; Zhang, X.; Lohse, D. Stability of Surface Nanobubbles: A Molecular Dynamics Study. *Langmuir* **2016**, *32* (43), 11116–11122.

(21) Yasui, K.; Tuziuti, T.; Kanematsu, W.; Kato, K. Dynamic Equilibrium Model for a Bulk Nanobubble and a Microbubble Partly Covered with Hydrophobic Material. *Langmuir* **2016**, *32* (43), 11101–11110.

(22) Nirmalkar, N.; Pacek, A. W.; Barigou, M. Bulk Nanobubbles from Acoustically Cavitated Aqueous Organic Solvent Mixtures. *Langmuir* **2019**, *35* (6), 2188–2195.

(23) Attard, P. The Stability of Nanobubbles. *Eur. Phys. J. Spec. Top.* **2014**, *223* (5), 1–22.

(24) Zhang, L.; Chen, H.; Li, Z.; Fang, H.; Hu, J. Long Lifetime of Nanobubbles Due to High Inner Density. *Sci. China Ser. G Physics, Mech. Astron.* **2008**, *51* (2), 219–224.

(25) Tan, B. H.; An, H.; Ohl, C.D. How Bulk Nanobubbles Might Survive. *Phys. Rev. Lett.* **2020**, *124* (13), 134503.

(26) Meegoda, J. N.; Hewage, S. A.; Batagoda, J. H. Application of the Diffused

Double Layer Theory to Nanobubbles. *Langmuir* **2019**, *35* (37), 12100–12112.

(27) Nirmalkar, N.; Pacek, A. W.; Barigou, M. Interpreting the Interfacial and Colloidal Stability of Bulk Nanobubbles. *Soft Matter* **2018**, *14* (47), 9643–9656.

(28) Ke, S.; Xiao, W.; Quan, N.; Dong, Y.; Zhang, L.; Hu, J. Formation and Stability of Bulk Nanobubbles in Different Solutions. *Langmuir* **2019**, *35* (15), 5250–5256.

(29) Jin, F.; Li, J.; Ye, X.; Wu, C. Effects of PH and Ionic Strength on the Stability of Nanobubbles in Aqueous Solutions of α-Cyclodextrin. *J. Phys. Chem. B* **2007**, *111* (40), 11745–11749.

(30) Dressaire, E.; Bee, R.; Bell, D. C.; Lips, A.; Stone, H. A. Interfacial Polygonal Nanopatterning of Stable Microbubbles. *Science* **2008**, *320* (5880), 1198 LP – 1201.

(31) Cho, S.H.; Kim, J.Y.; Chun, J.H.; Kim, J.D. Ultrasonic Formation of Nanobubbles and Their Zeta-Potentials in Aqueous Electrolyte and Surfactant Solutions. *Colloids Surfaces A Physicochem. Eng. Asp.* **2005**, *269* (1), 28–34.

(32) Parhizkar, M.; Edirisinghe, M.; Stride, E. The Effect of Surfactant Type and Concentration on the Size and Stability of Microbubbles Produced in a Capillary Embedded T-Junction Device. *RSC Adv.* **2015**, *5* (14), 10751–10762.

(33) Li, M.; Ma, X.; Eisener, J.; Pfeiffer, P.; Ohl, C.D.; Sun, C. How Bulk Nanobubbles Are Stable over a Wide Range of Temperatures. *J. Colloid Interface Sci.* **2021**, *596*, 184–198.

(34) Seddon, J. R. T.; Lohse, D.; Ducker, W. A.; Craig, V. S. J. A Deliberation on

Nanobubbles at Surfaces and in Bulk. *ChemPhysChem* **2012**, *13* (8), 2179–2187.

(35) Bunkin, N. F.; Shkirin, A. V; Suyazov, N. V; Babenko, V. A.; Sychev, A. A.; Penkov, N. V; Belosludtsev, K. N.; Gudkov, S. V. Formation and Dynamics of Ion-Stabilized Gas Nanobubble Phase in the Bulk of Aqueous NaCl Solutions. *J. Phys. Chem. B* **2016**, *120* (7), 1291–1303.

(36) Bui, T. T.; Nguyen, D. C.; Han, M. Average Size and Zeta Potential of Nanobubbles in Different Reagent Solutions. *J. Nanoparticle Res.* **2019**, *21* (8), 173.

(37) Uchida, T.; Liu, S.; Enari, M.; Oshita, S.; Yamazaki, K.; Gohara, K. Effect of NaCl on the Lifetime of Micro- and Nanobubbles. *Nanomaterials* . 2016.

(38) Hewage, S. A.; Kewalramani, J.; Meegoda, J. N. Stability of Nanobubbles in Different Salts Solutions. *Colloids Surfaces A Physicochem. Eng. Asp.* **2021**, *609*, 125669.

(39) Weijs, J. H.; Seddon, J. R. T.; Lohse, D. Diffusive Shielding Stabilizes Bulk Nanobubble Clusters. *ChemPhysChem* **2012**, *13* (8), 2197–2204.

(40) Plimpton, S. Fast Parallel Algorithms for Short-Range Molecular Dynamics. *J. Comput. Phys.* **1995**, *117* (1), 1–19.

(41) Stukowski, A. Visualization and Analysis of Atomistic Simulation Data with OVITO–the Open Visualization Tool. *Model. Simul. Mater. Sci. Eng.* **2009**, *18* (1), 15012.

(42) Weigend, F.; Ahlrichs, R. Balanced Basis Sets of Split Valence, Triple Zeta

Valence and Quadruple Zeta Valence Quality for H to Rn: Design and Assessment of Accuracy. *Phys. Chem. Chem. Phys.* **2005**, *7* (18), 3297–3305.

(43) Frisch, M. J.; Trucks, G. W.; Schlegel, H. B.; Scuseria, G. E.; Robb, M. A.; Cheeseman, J. R.; Scalmani, G.; Barone, V.; Petersson, G. A.; Nakatsuji, H. et al. Gaussian 16, Revision C.01. 2016.

(44) Becke, A. D. Density-functional Thermochemistry. III. The Role of Exact Exchange. *J. Chem. Phys.* **1993**, *98* (7), 5648–5652.

(45) Lee, C.; Yang, W.; Parr, R. G. Development of the Colle-Salvetti Correlation-Energy Formula into a Functional of the Electron Density. *Phys. Rev. B* **1988**, *37* (2), 785–789.

(46) Grimme, S.; Ehrlich, S.; Goerigk, L. Effect of the Damping Function in Dispersion Corrected Density Functional Theory. *J. Comput. Chem.* **2011**, *32* (7), 1456–1465.

(47) Kolev, N. I. Solubility of O_2, N_2, H_2 and CO_2 in Water BT - Multiphase Flow Dynamics 4: Turbulence, Gas Adsorption and Release, Diesel Fuel Properties; Kolev, N. I., Ed.; Springer Berlin Heidelberg: Berlin, Heidelberg, 2012; pp 209–239.

(48) Huang, T.W.; Liu, S.Y.; Chuang, Y.J.; Hsieh, H.Y.; Tsai, C.Y.; Wu, W.J.; Tsai, C.T.; Mirsaidov, U.; Matsudaira, P.; Chang, C.S. et al. Dynamics of Hydrogen Nanobubbles in KLH Protein Solution Studied with in Situ Wet-TEM. *Soft Matter* **2013**, *9* (37), 8856–8861.

(49) Zhou, L.; Wang, X.; Shin, H.J.; Wang, J.; Tai, R.; Zhang, X.; Fang, H.; Xiao, W.;

Wang, L.; Wang, C.; Gao, X. et al. Ultrahigh Density of Gas Molecules Confined in Surface Nanobubbles in Ambient Water. *J. Am. Chem. Soc.* **2020**, *142* (12), 5583–5593.

(50) Kang, B.; Tang, H.; Zhao, Z.; Song, S. Hofmeister Series: Insights of Ion Specificity from Amphiphilic Assembly and Interface Property. *ACS Omega* **2020**, *5* (12), 6229–6239.

(51) Hribar, B.; Southall, N. T.; Vlachy, V.; Dill, K. A. How Ions Affect the Structure of Water. *J. Am. Chem. Soc.* **2002**, *124* (41), 12302–12311.

(52) Manciu, M.; Ruckenstein, E. Specific Ion Effects via Ion Hydration: I. Surface Tension. *Adv. Colloid Interface Sci.* **2003**, *105* (1), 63–101.

(53) Ruckenstein, E.; Manciu, M. Specific Ion Effects via Ion Hydration: II. Double Layer Interaction. *Adv. Colloid Interface Sci.* **2003**, *105* (1), 177–200.

(54) Manciu, M.; Ruckenstein, E. On the Interactions of Ions with the Air/Water Interface. *Langmuir* **2005**, *21* (24), 11312–11319.

(55) Bauduin, P.; Nohmie, F.; Touraud, D.; Neueder, R.; Kunz, W.; Ninham, B. W. Hofmeister Specific-Ion Effects on Enzyme Activity and Buffer PH: Horseradish Peroxidase in Citrate Buffer. *J. Mol. Liq.* **2006**, *123* (1), 14–19.

(56) Marcus, Y. Effect of Ions on the Structure of Water: Structure Making and Breaking. *Chem. Rev.* **2009**, *109* (3), 1346–1370.

(57) Metrick, M. A.; do Carmo Ferreira, N.; Saijo, E.; Hughson, A. G.; Kraus, A.; Orrú, C.; Miller, M. W.; Zanusso, G.; Ghetti, B.; Vendruscolo, M. et al. Million-Fold

Sensitivity Enhancement in Proteopathic Seed Amplification Assays for Biospecimens by Hofmeister Ion Comparisons. *Proc. Natl. Acad. Sci.* **2019**, *116* (46), 23029 LP – 23039.

(58) Collins, K. D. Charge Density-Dependent Strength of Hydration and Biological Structure. *Biophys. J.* **1997**, *72* (1), 65–76.

(59) Timko, J.; Bucher, D.; Kuyucak, S. Dissociation of NaCl in Water from Ab Initio Molecular Dynamics Simulations. *J. Chem. Phys.* **2010**, *132* (11), 114510.

(60) Bouazizi, S.; Nasr, S.; Jaîdane, N.; Bellissent-Funel, M.C. Local Order in Aqueous NaCl Solutions and Pure Water: X-Ray Scattering and Molecular Dynamics Simulations Study. *J. Phys. Chem. B* **2006**, *110* (46), 23515–23523.

(61) Gaiduk, A. P.; Zhang, C.; Gygi, F.; Galli, G. Structural and Electronic Properties of Aqueous NaCl Solutions from Ab Initio Molecular Dynamics Simulations with Hybrid Density Functionals. *Chem. Phys. Lett.* **2014**, *604*, 89–96.

(62) Luzar, A.; Chandler, D. Effect of Environment on Hydrogen Bond Dynamics in Liquid Water. *Phys. Rev. Lett.* **1996**, *76* (6), 928–931.

(63) Ferrell, R. T.; Himmelblau, D. M. Diffusion Coefficients of Nitrogen and Oxygen in Water. *J. Chem. Eng. Data* **1967**, *12* (1), 111–115.

(64) Mills, R. Self-Diffusion in Normal and Heavy Water in the Range 1-45.Deg. *J. Phys. Chem.* **1973**, *77* (5), 685–688.

(65) Ding, Y.; Hassanali, A. A.; Parrinello, M. Anomalous Water Diffusion in Salt Solutions. *Proc. Natl. Acad. Sci.* **2014**, *111* (9), 3310 LP – 3315.

(66) Gowers, R. J.; Carbone, P. A Multiscale Approach to Model Hydrogen Bonding: The Case of Polyamide. *J. Chem. Phys.* **2015**, *142* (22), 224907.